λ*DNN:* Achieving Predictable Distributed DNN Training with Serverless Architectures

Fei Xu, *Member, IEEE*, Yiling Qin, Li Chen, *Member, IEEE*, Zhi Zhou, *Member, IEEE*, Fangming Liu, *Senior Member, IEEE*

Abstract—Serverless computing is becoming a promising paradigm for training distributed deep neural network (DDNN) in the cloud, as it allows users to decompose complex model training into a number of *functions* without managing virtual machines or servers. Though provided with a simpler resource interface (*i.e.*, function number and memory size), inadequate function resource provisioning (either under-provisioning or over-provisioning) easily leads to *unpredictable* DDNN training performance in serverless platforms. Our empirical studies on AWS Lambda indicate that, such *unpredictable performance* of serverless DDNN training is mainly caused by the resource bottleneck of parameter servers (PS) and small local batch size. In this paper, we design and implement λ*DNN*, a cost-efficient function resource provisioning framework to provide predictable performance for serverless DDNN training workloads, while saving the budget of provisioned functions. Leveraging the PS network bandwidth and function CPU utilization, we build a *lightweight* analytical DDNN training performance model to enable our design of λ*DNN* resource provisioning strategy, so as to guarantee DDNN training performance with serverless functions. Extensive prototype experiments on AWS Lambda and complementary trace-driven simulations demonstrate that, λ*DNN* can deliver predictable DDNN training performance and save the monetary cost of function resources by up to 66.7%, compared with the state-of-the-art resource provisioning strategies, yet with an acceptable runtime overhead.

Index Terms—Distributed DNN training, serverless computing, predictable performance, function resource provisioning.

1 Introduction

DISTRIBUTED Deep Neural Network (DDNN) training is becoming an increasingly important workload in the cloud [1]. As the DNN models get complex and datasets grow large, DDNN training workloads require a considerable amount of cloud resources and thus become computationally expensive [2]. To reduce the budget and ease the management of cloud resources, the serverless architecture has recently emerged as a promising paradigm for training DNN models in a distributed manner, as it allows cloud users to decompose complex model training into a number of *functions*, without managing virtual machines (VMs) or servers [3]. Most cloud providers have launched serverless platforms (*e.g.*, AWS Lambda [4], Google Cloud Functions [5], and Microsoft Azure Functions [6]) for commercial use such as machine learning, data processing, and Web applications. They offer cloud users a simple resource interface to specify the number and memory size of functions and then charge only for the consumed function resources [7]. As a result, it becomes increasingly compelling to deploy DDNN training workloads in serverless platforms.

Though users are offered a simple and flexible resource model in serverless platforms, serverless DDNN training workloads easily suffer from *unpredictable performance* [8], due to inadequate function resource provisioning (*under-provisioning* or *over-provisioning*). While under-provisioning (*e.g.*, insufficient function memory size) will automatically trigger several rounds of workload re-executions [9], over-provisioning can severely degrade the resource utilization of functions. The intrinsic function resource limitations (*e.g.*, function timeout) as listed in Table 1 can further deteriorate the training performance of large DNN models. As evidenced by our motivation experiment in Sec. 2.2, the CPU utilization of functions for training the MobileNet model can be drastically degraded from 92.1% to 25.7%. Such severe function CPU under-utilization mainly originates from: (1) *resource bottleneck of parameter servers (PS)* [2] and (2) *small local batch size* [10], though the functions have been well isolated (and thus little performance interference exists among functions) in public serverless platforms [11] (as evidenced by Sec. 2.2). Accordingly, the unpredictable performance elaborated above undoubtedly hinders cloud users from migrating DDNN training workloads to serverless platforms.

To solve such performance issues, many efforts have been devoted to optimizing the function performance *from the provider's perspective*. While most of them focus on enforcing isolation among functions (*e.g.*, FAASM [12]) or mitigating the cold-start latency (*e.g.*, Catalyzer [13]), comparatively little attention has been paid to *guaranteeing* the

- *Fei Xu, Yiling Qin are with the Shanghai Key Laboratory of Multidimensional Information Processing, School of Computer Science and Technology, East China Normal University, 3663 N. Zhongshan Road, Shanghai 200062, China. Email:* fxu@cs.ecnu.edu.cn.
- *Li Chen is with the Department of Computer Science, University of Louisiana at Lafayette, 301 East Lewis Street, Lafayette, LA 70504, USA. E-mail:* li.chen@louisiana.edu.
- *Zhi Zhou is with the Guangdong Key Laboratory of Big Data Analysis and Processing, School of Data and Computer Science, Sun Yat-sen University, 132 E. Waihuan Road, Guangzhou 510006, China. E-mail:* zhouzhi9@mail.sysu.edu.cn.
- *Fangming Liu is with the National Engineering Research Center for Big Data Technology and System, the Services Computing Technology and System Lab, Cluster and Grid Computing Lab, School of Computer Science and Technology, Huazhong University of Science and Technology, 1037 Luoyu Road, Wuhan 430074, China. E-mail:* fmliu@hust.edu.cn.

Manuscript received July XX, 2020; revised September XX, 2020.

performance [14] of serverless applications. There have also been several recent works on improving the cost efficiency of function resources for serverless applications *from the user's perspective*, such as machine learning inference [15] and training [16] as well as Spark jobs [17]. However, they mainly leverage existing machine learning algorithms like Deep Reinforcement Learning (DRL) [16] and Bayesian Optimization [18] to find a feasible amount of function resources. Such *black-box* approaches still require efforts (*i.e.*, around hundreds of iterations and high-quality profiled performance data samples) to train the model and thus bring non-negligible performance overhead. Moreover, the existing methods are not readily available for serverless DDNN training especially with large models (*e.g.*, ResNet50) due to the resource limitations of functions (*e.g.*, function timeout) listed in Table 1. As a result, there has been a paucity of research attention paid to delivering predictable performance to *long-running* DDNN training workloads in a *lightweight* manner in serverless platforms.

To fill this gap, in this paper, we present *λDNN*, a cost-efficient function resource provisioning framework to minimize the monetary cost and guarantee the performance for DDNN training workloads in serverless platforms. To the best of our knowledge, *λDNN* is the first attempt to demonstrate how to *achieve predictable performance for DDNN training workloads with serverless functions, while saving the training budget for cloud users. λDNN* can also reduce the resource cost for serverless computing providers. Specifically, we make the following contributions in *λDNN* as below.

▷ *First*, we build a serverless DDNN training framework with the PS architecture [19], and we design a *lightweight* analytical model to predict the DDNN training performance in serverless platforms. To capture the performance degradation caused by the resource bottleneck of PS and small local batch size, our model explicitly takes the PS network bandwidth and function CPU utilization into account.

▷ *Second*, we devise a *cost-efficient* function resource provisioning strategy to guarantee the performance of serverless DDNN training workloads. Given a DNN model with the training dataset and objective training time, *λDNN* first calculates the upper and lower bounds of provisioned functions, and then identifies an appropriate function resource provisioning plan (*i.e.*, the number and memory size of functions) with the minimal cost for DDNN training workloads.

▷ *Finally*, we implement a prototype of *λDNN* on AWS Lambda [4] and conduct extensive prototype experiments and large-scale trace-driven simulations with four representative DNN models. Experiment results show that *λDNN* can provide predictable performance for serverless DDNN training workloads, while reducing the monetary cost by up to 66.7%, in comparison to the state-of-the-art function resource provisioning strategies (*e.g.*, Siren [16]).

The rest of the paper is organized as follows. Sec. 2 empirically analyzes the key factors that cause unpredictable DDNN training performance in serverless platforms, which motivate the design of our analytical performance model for serverless DDNN training workloads in Sec. 3. Sec. 4 further presents the design and implementation of our *λDNN* function resource provisioning strategy. Sec. 5 evaluates the effectiveness and runtime overhead of *λDNN*. Sec. 6 discusses related work and Sec. 7 concludes this paper.

TABLE 1: Resource limitations of functions in the three representative serverless computing platforms.

Resources	Limitations		
	AWS	Google	Azure
#maximum memory (MB)	$3,008$	$2,048$	$1,536$
Timeout (seconds)	900	540	600
Local storage (MB)	512	> 512	1024

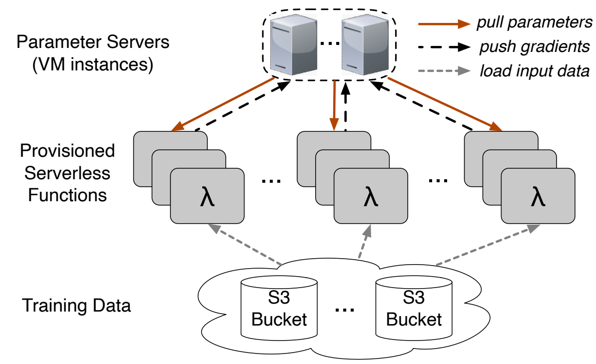

Fig. 1: A serverless DDNN training framework with the PS architecture in AWS Lambda [4].

2 Background and Motivation

In this section, we seek to understand the following questions: *how can we effectively train DNN models in a distributed manner in serverless platforms, and what are the key factors that impact the performance of serverless DDNN training workloads?*

2.1 DDNN Training with Serverless Functions

To reduce the complexity of DDNN training and ease the resource management in the cloud [20], deploying DDNN training workloads on serverless functions becomes increasingly compelling. However, DDNN training with serverless functions is challenging, mainly because the functions have stringent limitations on a set of resources such as memory size, lifetime, local storage. As listed in Table 1, each function is allocated with a flexible amount of memory with a maximum size. For instance, users are allowed to allocate function memory from 128 MB to $3,008$ MB with 64 MB increment step, and AWS Lambda [4] allocates *proportional* computing resources (*i.e.*, CPU capability, disk I/O bandwidth). The functions are invoked and scaled automatically by requests, and each function is terminated when it completes the user request or reaches the maximum execution time (*i.e.*, timeout). In addition, the function is "stateless" and the temporary local storage will be deleted when the function is terminated.

To effectively train the DNN model, we build a serverless DDNN training framework in a public cloud platform (*i.e.*, AWS Lambda [4]) as shown in Fig. 1. We adopt the PS architecture due to two facts. *First*, the PS architecture has been widely used in production machine learning clusters [19]. *Second*, serverless functions are not allowed to communicate with each other directly, which makes another widely-adopted Ring-AllReduce training architecture nontrivial to implement in serverless platforms [20]. Accordingly, to efficiently aggregate the gradients collected from functions

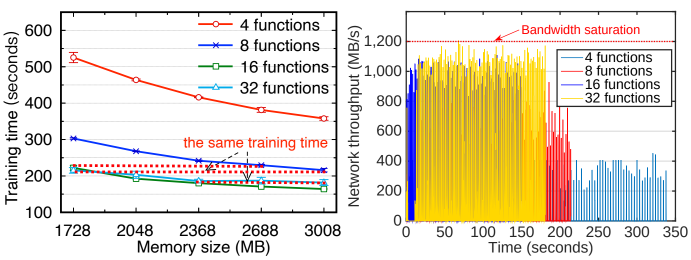

(a) (b)

Fig. 2: (a) Training time of the MobileNet model and (b) network throughput of PS over time, under different provisioning plans of function resources (*i.e.*, number and memory size of functions).

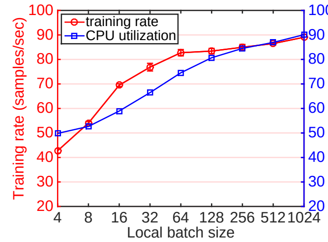

Fig. 3: Characterizing the relationship between the training rate, CPU utilization of a *single* function and *local* batch size for MobileNet.

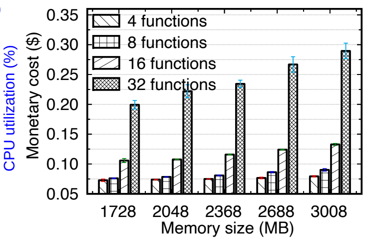

Fig. 4: Monetary cost of functions under different resource provisioning plans for training the MobileNet model.

TABLE 2: Average CPU utilization and network throughput of a function (*i.e.*, worker) during the training period of the MobileNet model under different resource provisioning plans.

Resource provisioning plans		CPU	Network
#functions (#batch)	#memory	utilization	throughput
4 functions (*local batch size:* 256)	$1,728$ MB	92.1%	3.85 MB/s
	$2,368$ MB	84.4%	3.95 MB/s
	$3,008$ MB	79.7%	4.08 MB/s
16 functions (*local batch size:* 64)	$1,728$ MB	70.0%	9.03 MB/s
	$2,368$ MB	60.8%	9.08 MB/s
	$3,008$ MB	53.0%	8.98 MB/s
32 functions (*local batch size:* 32)	$1,728$ MB	46.6%	7.56 MB/s
	$2,368$ MB	38.1%	7.59 MB/s
	$3,008$ MB	25.7%	7.65 MB/s

(*i.e.*, workers), we simply use VM instances with sufficient resources as the PS. In more detail, the training input data are initially stored in the distributed storage (*e.g.*, Amazon S3 [21]). The data are evenly partitioned and dispatched to the provisioned functions when the training of DNN model starts. For each iteration, the functions first calculate and push the model gradients to the PS for aggregation. The PS then updates the model parameters once it has received all the model gradients. Finally, the functions pull the updated model parameters from the PS for the next training iteration. In particular, the workers communicate with the PS through TCP connections. The training process above is iteratively executed, until the training loss reaches an objective value or a given number of training epochs have been processed [22].

Though serverless computing can ease the resource management and scaling, *how to provision the number and memory size of functions to guarantee the performance of serverless DDNN training* still remains challenging, even for a cloud expert. As DDNN training workloads commonly consume lots of computing resources, cloud users rely on their own experience to provision an adequate number of functions always with the largest-size memory (*i.e.*, $3,008$ MB) [20] to serverless deep learning workloads. Nevertheless, such a *naive* provisioning strategy [20] is likely to *underutilize* the function resources (*i.e.*, CPU, memory, I/O), thereby leading to *cost inefficiency* of function resource provisioning.

2.2 Characterizing Performance of Serverless DDNN Training Workloads

To explore the key factors that influence the performance of serverless DDNN training workloads, we conduct our motivation experiments by training representative DNN models (*e.g.*, MobileNet [23], ResNet50 [24]) on TensorFlow 1.3.1 using AWS Lambda functions [4]. Specifically, we launch a cluster of functions in the AWS region of N. Virginia (*i.e.*, `us-east-1`). We vary the number of provisioned functions from 4 to 32, and the function memory size from $1,728$ MB (*i.e.*, the minimum memory size to train the MobileNet model) to $3,008$ MB. To achieve fast convergence of DNN model training, we fix the *global batch size* as $1,024$, and the number of training iterations as 100 (*i.e.*, 2 epochs).

Performance of serverless DDNN training: As shown in Fig. 2(a), we observe that: *First*, the DDNN training time decreases as a larger amount of memory is allocated to functions. This is simply because a larger function memory size indicates more CPU cycles to process DDNN training workloads [4]. *Second*, provisioning more functions can expectedly speed up the DDNN training process. *Interestingly*, 16 and 32 functions have a *slower* improvement in DDNN training performance compared with 4 and 8 functions. Moreover, 32 functions slightly increase the DDNN training time compared to 16 functions when allocated with over $2,048$ MB memory. We conjecture that: as more functions (*i.e.*, 16, 32 functions) are provisioned, **(a)** the network I/O bandwidth of PS becomes *bottleneck*, and **(b)** a *smaller local batch size* of training data is processed on each function, as well as **(c)** the performance interference of functions *might* become severe [8]. The three factors above inevitably *underutilize* the CPU resource of provisioned functions (as shown in Table 2), and thus *offset* the performance gains of increased function resources.

Resource bottleneck of PS: To verify our analysis above, we further examine the system-level metrics including CPU utilization and network throughput of functions and PS with different resource provisioning plans. Specifically, we normalize the CPU utilization of functions by dividing the measured utilization data (*i.e.*, executing the `top` command every 0.5 seconds) to the allocated proportion of CPU capacity (*e.g.*, $3,008$ MB memory corresponds to $\frac{3,008}{1,792\times 2} = 0.839$ of CPU capacity). Also, we measure the network throughput of PS and functions by tracing the network I/O statistics in the `proc` file system. As listed in Table 2, we observe that the function CPU utilization gradually decreases from 92.1% to 25.7% as more function resources are provisioned. This implies that the PS network bandwidth becomes *bottleneck* as more functions are provisioned, which is evidenced by Fig. 2(b) that the PS bandwidth becomes saturated at around $1,200$ MBps for over 16 functions. Moreover, our measurement study shows that the network throughput of functions *surprisingly remains unchanged* as the amount of allocated function memory increases (from $1,152$ to $3,008$ MB in Table 2). As a result, the data communication becomes dominating the serverless DDNN training process as the more function resources are provisioned, which in turn degrades the CPU utilization of functions.

Small local batch size: As more functions are provisioned, the *fixed global batch size* can lead to a *smaller local batch size* per function, thereby degrading the training rate on each function [10]. To verify that, we examine the function training rate and CPU utilization of the MobileNet model trained on a single function which connects to a PS node. As shown in Fig. 3, the function training rate gradually converges to a peak value (*i.e.,* 90 samples/sec) as the local batch size increases, which is highly related to the CPU utilization of a function. As the local batch size gets smaller (*i.e.,* less than 64), it *negatively* degrades the function CPU utilization below 80%. Accordingly, it would be challenging to find local and global batch sizes *good* enough to achieve both fast training rate and model convergence.

Performance interference of functions: We experimentally examine the severity of performance interference [8] among functions. Specifically, we launch 200 different AWS Lambda functions with 128 MB memory, and then use the `sysbench` benchmark to measure the CPU, memory and disk I/O performance of functions. *Surprisingly,* we identify stable function performance and thus the performance variation can be negligible among functions (*e.g.,* the average function written throughput is 12.78 MB/s with a negligible standard deviation of 0.60). We further run the `uname` command in functions to obtain the underlying host VM's IP [25]. We find that all these 200 Lambda functions have different host VM's IPs, which implies that these functions are distributed among different VMs (*i.e.,* not colocated). Our experimental results above are consistent with a latest work [11], which reports that AWS Lambda [4] has recently launched a lightweight VM monitor named Firecracker [11] to significantly mitigate the performance interference and achieve isolation among functions.

Monetary cost of serverless DDNN training: As analyzed above, we conclude that *blindly over-provisioning more function resources can be cost-inefficient*. As shown in Fig. 4, the largest memory allocation (*i.e.,* $3,008$ MB) increases the monetary cost by 45.3% compared to the lowest memory allocation (*i.e.,* $1,728$ MB) when allocated with 32 functions, while the training time is reduced only by 18.4%. This is mainly because the function resources are *underutilized* (*i.e.,* wasted) as analyzed in Table 2. *Interestingly*, 8 functions with $2,688$ memory and $3,008$ memory have almost the same DDNN training performance with 16 functions and 32 functions with $1,728$ memory (as shown in Fig. 2(a)), respectively, but the former resource provisioning plans can reduce 22.5-121.1% of monetary cost over the latter ones. This brings us an opportunity to judiciously provision function resources to serverless DDNN training workloads, with the aim of *guaranteeing the objective DDNN training performance while minimizing the monetary cost.*

An illustrative example: To achieve predictable serverless DDNN training performance and *cost-efficient* resource provisioning of functions, we propose λ*DNN* in Sec. 4 and illustrate its effectiveness by conducting another motivation experiment with the ResNet50 model [24]. We train the model with one epoch and set the objective DDNN training time of 600 seconds. As listed in Table 3, the random strategy randomly selects 4 functions allocated with $1,536$ MB memory and it fails to train the ResNet50 model. This is because the allocated function resources of $1,536$ MB are too small to process the training of ResNet50. Though the naive strategy [20] choose the largest memory size, it exceeds the objective training time by 17.3% with the highest budget, as it chooses an inadequate small local batch size. Siren [16] and λ*DNN* both can train the workload within the objective training time, but Siren [16] causes a higher monetary cost by 13.9% compared with our λ*DNN* strategy. As a result, our λ*DNN* strategy can finish the DDNN training within the objective training time in a cost-efficient manner.

TABLE 3: Comparison of the ResNet50 model training time and monetary cost of resources with different function provisioning strategies.

Strategies	Provisioning plans		Time	Cost
	#functions (#batch)	#memory	(seconds)	(10^{-2}\$)
Random	4 (*local batch:* 64)	$1,536$ MB	Failure	N/A
Naive [20]	8 (*local batch:* 64)	$3,008$ MB	703.95	29.40
Siren [16]	9 (*local batch:* 128)	$2,816$ MB	528.96	23.19
λ*DNN*	8 (*local batch:* 128)	$2,560$ MB	**573.34**	**20.36**

Summary: *First,* the serverless DDNN training performance is essentially determined by the PS network bandwidth and function CPU utilization. In particular, the resource bottleneck of PS and small local batch size are the main factors that underutilize the function resources and thus slow down the training rate. *Second,* judiciously optimizing the resource provisioning of serverless functions can achieve significant cost saving while delivering predictable performance for DDNN training workloads.

3 Modeling DDNN Training Performance in Serverless Platforms

In this section, we first build an *analytical* model to predict the serverless DDNN training performance, by explicitly considering the network bandwidth of PS and CPU utilization of provisioned functions. Next, we formulate the function resource provisioning problem to minimize the monetary cost with an objective DDNN training time, and then analyze the problem complexity. The key notations in our performance model are summarized in Table 4.

3.1 Predicting DDNN Training Time with Serverless Function Resources

Serverless DDNN training can be divided into *data loading* process and *model training* process, as illustrated in Fig. 1. Specifically, each function (*i.e.,* worker) first fetches a batch of training data samples from Amazon S3 storage. Then, the functions *iteratively* calculate the model gradients based on a batch of fetched data samples, and upload the computed model gradients to the PS where the gradients from all functions are aggregated. Finally, the functions download the updated model parameters from the PS to complete one training iteration. In general, the DNN model requires a

TABLE 4: Key notations in our serverless function-based DDNN training performance model.

Notation	Definition
B_f^p	Available network bandwidth between a function and PS
B_f^s	Available network bandwidth between a function and S3
B_p	Network bandwidth of the PS nodes
B_s	Disk I/O bandwidth of the S3 storage
R	Training rate of a single function
m	Allocated function memory size
n	Number of provisioned functions
b_l, b_g	Local, global batch size of training data samples
d_t, n_t	Size, number of training data samples
d_m	Size of model parameters and model gradients
k, e	Number of training iterations, epochs
t_{comp}	Computation time for each training iteration
t_{comm}	Data communication time for each training iteration
t_{load}	Data loading time of training data samples

number of iterations (denoted by k) to converge to an objective training loss value. Accordingly, the DDNN training time T can be calculated by summing up the loading time t_{load} of data samples, and the computation time t_{comp} of model gradients, as well as the communication time t_{comm} of model parameters and gradients, which is given by

$$T = t_{load} + k \cdot (t_{comp} + t_{comm}). \tag{1}$$

Given the number of training data samples n_t, the number of training epochs e (where one epoch denotes the training of the whole n_t data samples), and the global batch size b_g, the number of training iterations k can be calculated by

$$k = \frac{n_t \cdot e}{b_g}. \tag{2}$$

Data loading process. To achieve fast convergence, we consider the data communication of functions follows Bulk Synchronous Parallel (BSP) protocol, which has been widely used in production machine learning clusters [19]. To effectively train the DNN model, we also simply assume that the training data samples are *evenly* partitioned across the provisioned functions. Accordingly, t_{load} is calculated as

$$t_{load} = \frac{d_t}{n \cdot B_f^s}, \tag{3}$$

where B_f^s denotes the available network bandwidth between the function and S3 storage. d_t is the size of training dataset and n denotes the number of provisioned functions.

Model training process. For each iteration, each provisioned function trains a set of data samples with the *local* batch size (denoted by b_l). Given a local batch size, the total number of data samples processed in one iteration (*i.e., global* batch size $b_g = b_l \cdot n$) gets larger as more functions are provisioned. Moreover, the training rate (*i.e.,* the processing rate of data samples, denoted by R) of a function is considered as the same over the iterations with the BSP protocol. Accordingly, given n provisioned functions, we estimate the computation time t_{comp} of model gradients as

$$t_{comp} = \frac{b_g}{n \cdot R} = \frac{b_l}{R}. \tag{4}$$

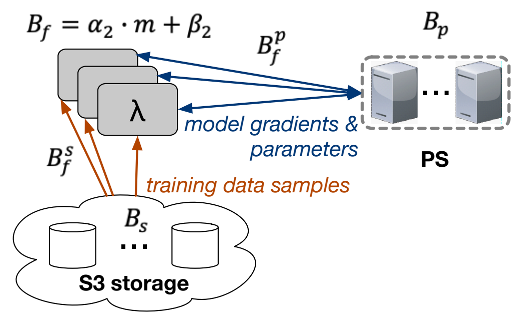

Fig. 5: Data communication between functions and PS nodes, as well as the training data loading between functions and S3.

In addition, the data communication time t_{comm} of each iteration includes the network transfer time to upload (push) model gradients to the PS and download (pull) the model parameters from the PS, as shown in Fig. 5. Given the size of model parameters d_m, which is practically the same as the size of model gradients [22], we can calculate the data communication time t_{comm} as

$$t_{comm} = \frac{2 \cdot d_m}{B_f^p}, \tag{5}$$

where B_f^p denotes the available network bandwidth between a function and PS nodes.

We proceed to model the training rate R of a single function and the network bandwidth (*i.e.,* B_f^p, B_f^s). As discussed in Sec. 2.1, the CPU capacity of functions is actually proportional to the allocated memory of functions [4]. Accordingly, the computation time is highly related to (*i.e.,* in proportion to) the function memory size m, as evidenced by Sec. 2.2. We formulate the training rate of a function as

$$R = \alpha_1 \cdot m + \beta_1, \tag{6}$$

where α_1 and β_1 are model coefficients. In particular, the network bandwidth B_f^p between a function and PS (*i.e.,* EC2 instances) is actually *independent* of the function memory as evidenced by our experiment results in Table 2. Accordingly, it is bounded by the PS network bandwidth for each function $\frac{B_p}{n}$, as the network bandwidth of PS can become *bottleneck* (as analyzed by Sec. 2.2). Meanwhile, the network bandwidth B_f^s between a function and S3 is linear to the function memory, and it is bounded by the I/O bandwidth of S3 storage B_s. As a result, we formulate B_f^p and B_f^s as

$$B_f^p = \min\left(B_f^{max}, \frac{B_p}{n}\right), \tag{7}$$

$$B_f^s = \min(B_f, B_s) = \min\left(\alpha_2 \cdot m + \beta_2, B_s\right), \tag{8}$$

where α_2 and β_2 are model coefficients, and B_f^{max} denotes the *fixed* network bandwidth between a function and an EC2 instance. By substituting Eq. (2) – Eq. (8) into Eq. (1), we find that the DDNN training time T is actually decided by the number n and memory size m of provisioned functions as well as the local batch size b_l, which is denoted by a triple $\langle n, m, b_l \rangle$. While simple, our model is *effective enough* to predict the serverless DDNN training performance. We will evaluate the model accuracy in Sec. 5.2.

Obtaining model parameters: Based on the above, the parameters of our DDNN training performance model include five *workload-specific* parameters d_t, n_t, d_m, α_i, β_i, and

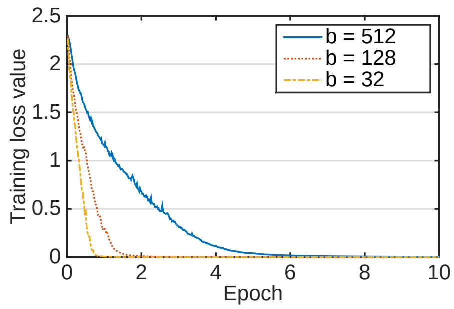

Fig. 6: Fitting training loss of `cifar10` DNN model with different global batch sizes (*e.g.*, $b_g = 512, 128, 32$).

three *platform-specific* parameters B_p, B_f^{max}, B_s. Specifically, the input dataset size d_t, the number of data samples n_t, and the model size d_m can be easily obtained, once the DDNN training workload (*i.e.*, the DNN model and training dataset) is submitted to the serverless platform. Furthermore, the model coefficients α_i, β_i in Eq. (6) and Eq. (8) can be obtained by workload profiling. Specifically, we profile (*i.e.*, train) the DNN model on a single one function with a small number (*i.e.*, 50) of iterations, and we record the training rates and the network bandwidth between the function and S3 under different function memory sizes. To acquire model coefficients, we fit the recorded data including the training rates and network bandwidth using the linear regression method [26]. In addition, the network bandwidth B_p and B_f^{max} can be measured running the `netperf` tool in an EC2 instance (*i.e.*, the PS node) and a function, respectively. The disk I/O bandwidth B_s of S3 storage can be obtained by transferring data from an EC2 instance to S3 by `AWS CLI`.

Identifying local and global batch sizes: To examine the relationship between DDNN training loss and global batch size, we collect the training loss values of `cifar10` DNN model[1] with six different global batch sizes (*i.e.*, 16, 32, 64, 128, 256, and 512). As shown in Fig. 6, the training loss highly depends on the number of epochs e and the global batch size b_g [22]. The model requires more epochs to reach an objective training loss value (*i.e.*, converges slowly), as b_g gets larger (when b_l is fixed and more functions are provisioned). To guarantee fast model convergence, we simply set a maximum global batch size b_g^{max} (*e.g.*, $1,024$) [10] for DDNN training. Meanwhile, we identify a local batch size b_l^f for the DNN model to achieve relatively high function CPU utilization (as evidenced by Sec. 2.2), as long as the global batch size (*i.e.*, $b_l^f \cdot n$) is below b_g^{max}. Accordingly, the local batch size b_l can be set as

$$b_l = \begin{cases} b_l^f & b_l^f \cdot n \le b_g^{max}, \\ \frac{b_g^{max}}{n} & \text{otherwise}. \end{cases} \tag{9}$$

We obtain b_l^f for each DNN model to achieve high function CPU utilization (*e.g.*, $\geq 80\%$) during the workload profiling on a single function.

1. The tutorial DNN model [27] defined in the project path "/models/tutorials/image/cifar10/" of Tensorflow.

3.2 Analyzing Resource Provisioning Optimization Problem of Serverless Functions

Based on our DDNN training performance model above, we further formulate the resource provisioning optimization problem of serverless functions. The objective is to minimize the monetary cost of provisioned function resources, while guaranteeing the performance of DDNN training workloads. Given the unit price of functions p and the objective DDNN training time T_o, our optimization problem is formally defined as

$$\min_{m,n} \quad C = m \cdot n \cdot p \cdot T \tag{10}$$

$$\text{s.t.} \quad T \le T_o, \tag{11}$$

$$m \in \{64 \cdot j | 2 \le j \le 47, j \in \mathbb{Z}^+\}, \tag{12}$$

$$n \in \mathbb{Z}^+, \tag{13}$$

where Eq. (10) defines our objective function which minimizes the monetary cost of function resource provisioning, subject to the following three constraints. Specifically, Constraint (11) guarantees the DDNN training time below the objective time T_o. Constraint (12) denotes that the allocated function memory is within the range from 128 MB to $3,008$ MB with the memory increment size of 64 MB. Constraint (13) indicates that the number of provisioned functions requires to be a positive integer.

Problem analysis: By substituting Eq. (1) – Eq. (9) into Eq. (10), the monetary cost C is actually affected by m and n. Obviously, the training time T in Constraint (11) and the monetary cost C is non-linear with m and n. Accordingly, our optimization problem turns out to be in the form of *non-linear integer programming*, which is NP-hard to solve [28]. We turn to design a heuristic algorithm in Sec. 4 to solve such a resource provisioning optimization problem.

To improve the algorithm efficiency, we proceed to analyze the lower bound n_{lower} and upper bound n_{upper} of provisioned functions. According to Eq. (7), the network bandwidth of functions can be *underutilized* as more functions are provisioned and thus saturates the PS network bandwidth. To avoid the resource bottleneck of PS and fully utilize the function resources (*i.e.*, CPU, network bandwidth), we have $\frac{B^p}{n} \geq B_f^{max}$. Accordingly, the upper bound of provisioned functions n_{upper} is calculated as

$$n_{upper} = \left\lfloor \frac{B^p}{B_f^{max}} \right\rfloor. \tag{14}$$

According to Constraint (11) (*i.e.*, $T \le T_o$), we substitute Eq. (3) – Eq. (5) into Eq. (1), and calculate the lower bound of provisioned functions n_{lower} as follows:

$$n_{lower} = \begin{cases} \left\lceil \frac{\lambda}{\kappa} + \frac{\mu}{b_l^f \cdot \kappa} \right\rceil & b_l^f \cdot n \le b_g^{max}, \\ \max\left(\left\lfloor \frac{b_g^{max}}{b_l^f} \right\rfloor, \left\lceil \frac{b_g^{max} \cdot \lambda}{b_g^{max} \cdot \kappa - \mu} \right\rceil \right) & \text{otherwise}, \end{cases} \tag{15}$$

where $\lambda = B_f^p \cdot (R \cdot d_t + n_t \cdot e \cdot B_f^s)$, $\kappa = T_o \cdot R \cdot B_f^s \cdot B_f^p$, and $\mu = 2 \cdot d_m \cdot n_t \cdot e \cdot B_f^s \cdot R$ denote the coefficients to calculate n_{lower}. In fact, two model parameters (*i.e.*, B_f^s, R) are the functions of m, according to Eq. (6) and Eq. (8). In more detail, when $n_{lower} > \frac{b_g^{max}}{b_l^f}$, it indicates that the objective training time T_o can only be achieved by fixing the global size as b_g^{max}, so that the model training convergence can be guaranteed. When $n_{upper} \leq \frac{b_g^{max}}{b_l^f}$, it implies that we can meet the objective training time by fixing the local batch size as b_l^f, while achieving high function utilization. As a result, we are able to narrow down the search space of provisioned functions within the range from n_{lower} to n_{upper} by Eq. (14) and Eq. (15), given an allocated function memory size m.

4 Design of λ*DNN*: Guaranteeing Performance of Serverless DDNN Training Workloads

Based on our serverless DDNN performance model and resource provisioning optimization problem defined in Sec. 3, we further present λ*DNN* in Alg. 1, a *simple yet effective* function resource provisioning strategy in the serverless platform (*e.g.*, AWS Lambda [4]). Our λ*DNN* strategy aims to provide predictable performance for serverless DDNN training workloads, while minimizing the monetary cost of function resource provisioning.

4.1 Algorithm Design

How does λ*DNN* work? Given a DDNN training workload (*i.e.*, the DNN model and training dataset) with the objective training time T_o and the number of training epochs e, λ*DNN* first initializes the number and allocated memory size of provisioned functions as well as the monetary cost. According to the parameter acquisition method elaborated in Sec. 3.1, λ*DNN* then obtains the *platform-specific* parameters (*i.e.*, B_p, B_f^{max}, B_s) and *model-specific* parameters (*i.e.*, α_i, β_i, b_l^f) through the workload profiling on a single function (lines 1-3). To speedup the algorithm execution, λ*DNN* also identifies the minimum function memory size m_{min} to train the DNN model, and it iteratively allocates the function memory size to the maximum of $3,008$ MB with the step of 64 MB (lines 4-5). For each allocated function memory size m_i, λ*DNN* further calculates the DDNN training rate R by Eq. (6), and the network bandwidth B_f^s between a function and S3 by Eq. (8). To narrow down the search space of the number of provisioned serverless functions, λ*DNN* proceeds to calculate the upper and lower bounds of n (lines 6-7). By iterating all the possible numbers of provisioned functions in the range from n_{lower} to n_{upper}, λ*DNN* is able to calculate the DDNN training time T by Eq. (1) and the monetary cost C using Eq. (10) (lines 8-9). Finally, λ*DNN* identifies the cost-efficient function resource provisioning plan including the number of serverless functions n and the allocated memory size m, with the guaranteed training time ($T \leq T_o$) and the minimum monetary cost (lines 10-13).

Remark: The complexity of Alg. 1 is in the order of $\mathcal{O}(p \cdot q)$, where $p = n_{upper} - n_{lower} + 1$ denotes the cardinality of search space of n, and q denotes the number of possible function memory sizes, which is less than $\frac{3,008-128}{64} + 1 = 46$ according to Constraint (12). The minimum function memory size m_{min} further improves the algorithm efficiency, as the DNN model size is large in common (*e.g.*, m_{min} is $2,432$ MB for ResNet50 [24]). Accordingly, the complexity of Alg. 1 is reduced to $\mathcal{O}(p)$, which indicates the computation overhead of our λ*DNN* strategy can be well controlled. In particular, λ*DNN* identifies a *sub-optimal* function resource provisioning plan, as we narrow down the search space of function numbers and memory sizes. We will validate the lightweight runtime overhead of λ*DNN* in Sec. 5.4.

Algorithm 1: λ*DNN:* Cost-efficient function resource provisioning strategy for predictable performance of serverless DDNN training workloads.

Input: DDNN training workload with its input dataset size d_t, number of data samples n_t, model size d_m, and the objective training time T_o and number of epochs e.
Output: Cost-efficient function resource provisioning plan (*i.e.*, the number n and memory size m of functions).

```
1:  Initialize: C_min ← ∞; m ← 0; n ← 0;
2:  Acquire platform-specific parameters B_p, B_f^max, and B_s;
3:  Obtain model-specific parameters α_i, β_i, and b_l^f, as well as
    the minimum memory size m_min to train the DNN model,
    through workload profiling on a single function;
4:  Set m_i ← m_min;
5:  while m_i ≤ 3,008 do
6:      Calculate the DDNN training rate R ← Eq. (6), and
        function network bandwidth B_f^s ← Eq. (8);
7:      Calculate the lower bound n_lower ← Eq. (15), and the
        upper bound n_upper ← Eq. (14);
8:      for all n_i in [n_lower, n_upper] do
9:          Calculate T ← Eq. (1), and C ← Eq. (10);
10:         if T ≤ T_o && C < C_min then
11:             Record the resource provisioning plan m ← m_i,
                n ← n_i, and its monetary cost C_min ← C;
12:             break;
13:         end if
14:     end for
15:     Set m_i ← m_i + 64;
16: end while
```

4.2 Implementation of λ*DNN*

We implement a prototype of λ*DNN* framework running on AWS Lambda [4], with over $1,500$ lines of Python, C++, and Linux Shell codes which are publicly available on GitHub[2]. To enable efficient network communication between the functions and PS, we adopt an open-source asynchronous messaging library ZeroMQ[3]. Specifically, λ*DNN* comprises two pieces of modules: a *training performance predictor* and a *function resource provisioner* as illustrated in Fig. 7. Specifically, users first submit a DDNN training workload (*i.e.*, the DNN model and training dataset) and the objective training time to the λ*DNN portal*, which can be deployed on either an EC2 instance or a Lambda function. With the model parameters obtained by λ*DNN portal*, the *performance predictor* then predicts the DDNN training time using our performance model designed in Sec. 3. To guarantee the objective DDNN training time, the *resource provisioner* further identifies the cost-efficient serverless function resource provisioning plan using Alg. 1 devised in Sec. 4. Once the cost-efficient resource provisioning plan is determined, the *function allocator* finally sets up a number of functions with an appropriate amount of memory using the command-line tools for serverless platforms (*e.g.*, `AWS CLI`).

Why to deploy λ*DNN*? The benefit of deploying λ*DNN* in serverless platforms is *twofold*. From the user's perspective, λ*DNN* can guarantee the DDNN training performance

2. https://github.com/icloud-ecnu/lambdadnn
3. https://zeromq.org

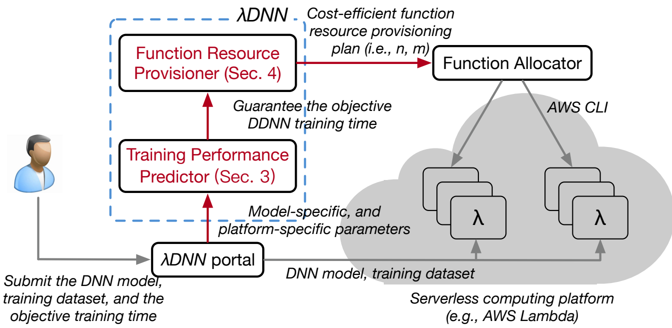

Fig. 7: λ*DNN* prototype in serverless computing platforms.

while saving the training budget. Accordingly, deploying λ*DNN* can attract the cloud users to migrating their DDNN training workloads to serverless platforms. From the provider's perspective, λ*DNN* can achieve the objective DDNN training time by provisioning less function resources compared with the state-of-the-art function resource provisioning strategies (*i.e.*, Siren [16]). As a result, λ*DNN* can reduce the resource cost to complete a DDNN training workload, thereby serving more DDNN training requests for a serverless computing platform. We will evaluate the benefits of λ*DNN* from both the perspectives of users and providers in Sec. 5.3.

We discuss two practical issues related to the implementation of λ*DNN* as follows. *First is how to deal with the timeout of serverless functions.* As illustrated in Table 1, the serverless functions are terminated once the function expires at a certain amount of time (*e.g.*, 900 seconds for Lambda functions), which brings unpredictable performance overhead to the *long-running* DDNN training workloads. λ*DNN* simply leverages the *proactive checkpointing* technique to mitigate such performance overhead in a lightweight manner. Specifically, λ*DNN* first leverages the performance model in Sec. 3 to predict the number of iterations k_{check} that can be successfully trained before the expiration of functions (*e.g.*, 30 seconds ahead of function expirations). After k_{check} iterations, λ*DNN* then proactively checkpoints the function state (*e.g.*, the current iteration number, local batch size, and model parameters) to the S3 storage [21]. Finally, the *function allocator* of λ*DNN* relaunches a set of functions to download the function states and training dataset from S3, and restores the DDNN training process. In particular, the function relaunch process is lightweight (*i.e.*, *warm start* [29]) as the relaunched functions can be online within several seconds in our experiments.

Second is how to train large DNN models in λ*DNN*. λ*DNN* currently supports *data parallelism*. It requires to be extended to support *model parallelism* when *extremely large* DNN models are trained in serverless functions. For instance, the VGG19 model (with the model size of 576 MB) generates too large temporary files to be stored in the /`tmp` directory of functions (with the storage limitation of 512 MB). Accordingly, the large DNN model requires splitting into several parts (*i.e.*, model parallelism) so that each part of the DNN model can be fitted in the function. We will extend λ*DNN* to support the model parallel training as our future work.

TABLE 5: Configurations and model-specific parameters of four representative DDNN training workloads.

Model	`cifar10` DNN	1DCNN	MobileNet	ResNet50
Dataset	`cifar10`	IMDB	`cifar10`	`cifar10`
#dataset (MB)	148	41.1	148	148
#model (MB)	0.64	2	18	98
b_l^f	64	32	64	128
b_g^{max}	512	512	512	1,024
α_1, β_1	0.3, 6.7	0.1, −8.8	0.03, 5.6	0.003, 11.3

5 Performance Evaluation

In this section, we evaluate λ*DNN* by carrying out a set of prototype experiments with four representative DNN models (listed in Table 5) trained on AWS Lambda [4], as well as large-scale simulations driven by Microsoft Azure traces [30]. Our prototype experiments and trace-driven simulations seek to answer the following questions:

- **Accuracy:** Can our λ*DNN* performance model accurately predict the performance of serverless DDNN training workloads? (Sec. 5.2)
- **Effectiveness:** Can our λ*DNN* resource provisioning strategy deliver predictable performance to serverless DDNN training workloads, while saving the monetary cost? (Sec. 5.2 & Sec. 5.3)
- **Overhead:** How much runtime overhead does λ*DNN* practically bring? (Sec. 5.4)

5.1 Experimental Setup

Configurations of serverless DDNN training cluster: We set up a serverless training cluster according to Fig. 1 in the `us-east-1` region. Specifically, we use an `m5.large` EC2 instance (equipped with 2 vCPUs, 8 GB memory) to serve as the PS, and the Lambda functions are served as the workers. We set up an S3 bucket to store the training dataset in `us-east-1` to save the budget. In particular, we measure the three *platform-specific* parameters (*i.e.*, B_p, B_f^{max}, B_s) using the `netperf` tool and `Boto3` SDK[4] according to Sec. 3.1. The network bandwidth of PS B_p and a function B_f^{max} is set as 1.2 GBps and 84 MBps, respectively, and the disk I/O bandwidth of S3 B_s is set as 115 MBps.

DDNN training workloads and datasets: We select four representative DNN models as listed in Table 5, which includes (1) the `cifar10` DNN model [27] for image classification, (2) the 1DCNN model [31] trained on the IMDB dataset for text classification, (3) the MobileNet model [23] trained on the `cifar10` dataset for image classification, (4) the ResNet50 model [24] trained on the `cifar10` dataset for image classification. Through workload profiling on a single function, we are able to obtain the key *model-specific* parameters as elaborated in Table 5.

Comparable function provisioning strategies and metrics: We compare λ*DNN* with the following two strategies: (1) Naive provisioning [20], which always provisions the largest memory size to functions and randomly chooses the number of functions for DDNN training workloads; (2) Modified Siren [16], which leverages the DRL method to

4. https://boto3.amazonaws.com/v1/documentation/api/latest/index.html

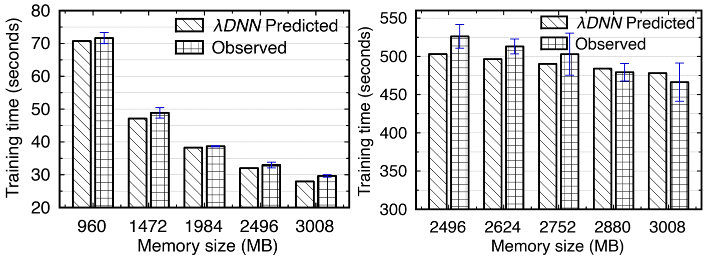

(a) (b)

Fig. 8: λDNN prediction for the training time of (a) 1DCNN model and (b) ResNet50 model with different function memory sizes.

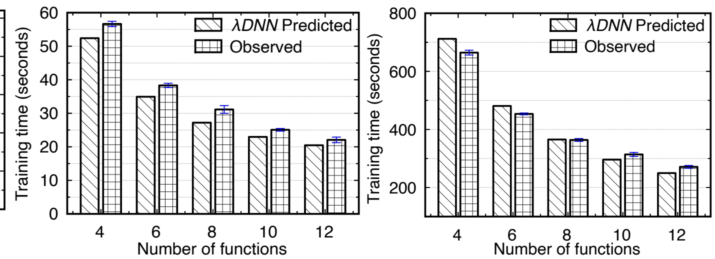

(a) (b)

Fig. 9: λDNN prediction for the training time of (a) `cifar10` DNN model and (b) MobileNet model with different numbers of provisioned functions.

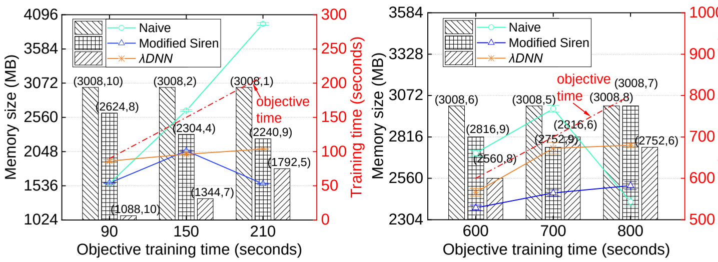

(a) (b)

Fig. 10: Comparison of provisioned function resources and the obtained DDNN training performance achieved by the naive, modified Siren, and λDNN strategies, for training 1DCNN model and ResNet50 model.

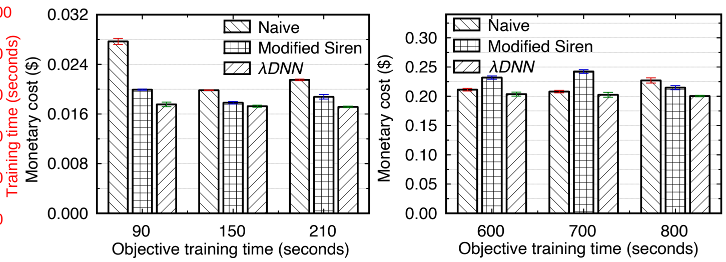

(a) (b)

Fig. 11: Comparison of monetary cost of provisioned function resources by the naive, modified Siren, and λDNN strategies for training 1DCNN model and ResNet50 model.

select the adequate number and memory size of functions for achieving predictable performance while minimizing the monetary cost of DDNN training workloads, as the stock Siren strategy [16] aims to reduce the DDNN training time given a budget. We focus on two key metrics including the DNN training time and the monetary cost for each resource provisioning plan. We illustrate the DDNN workload performance with error bars of standard deviation by repeating the DNN training workload for three times.

5.2 Effectiveness of λDNN

Can λDNN accurately predict the serverless DDNN training time? We first examine our λDNN predicted training time of 1DCNN and ResNet50 by varying the function memory size with a fixed number (*i.e.*, 8) of functions. Specifically, we train 1DCNN and ResNet50 for 3 epochs and 1 epoch, respectively. We start the minimum function memory size m_{min} as 960 MB for 1DCNN and $2,496$ MB for ResNet50, respectively. As shown in Fig 8, our performance model can well predict the DDNN training time with a prediction error of 0.98% – 6.0%, as the function memory increases to $3,008$ MB. Fig 8(a) depicts that our predicted training time of 1DCNN is basically faster than the observed time. This is because small DNN models ($d_m = 2$ MB for 1DCNN) cannot fully utilize the function network bandwidth, which makes our performance model overestimate the training performance especially for small DNN models. Moreover, Fig. 8(b) shows that λDNN first overestimates and then underestimates the training performance for ResNet50, which implies that our performance model is insensitive to the allocated function memory for ResNet50. This is because the serverless training performance of large DNN models is unstable with a large standard deviation (*i.e.*, up to 34.98 seconds), which inevitably makes our workload profiling inaccurate for ResNet50. To effectively train large DNN models in functions, we will extend λDNN to support model parallelism (*i.e.*, splitting models into several parts) of DDNN training, as discussed in Sec. 4.2.

We further examine the our λDNN predicted training time for `cifar10` DNN and MobileNet by varying the number of functions from 4 to 12 with a fixed amount of function memory (*i.e.*, $3,008$ MB). As depicted in Fig. 9, λDNN can basically predict the DDNN training performance with a prediction error of 0.43% – 14.48%, as the number of provisioned functions increases. Specifically, Fig. 9(a) shows that λDNN overestimates the DDNN training performance for `cifar10` DNN simply because its model size is small (*i.e.*, 640 KB) as discussed in Fig. 8(a). In particular, Fig. 9(b) illustrates that the prediction error of our performance model becomes large (from 0.43% to 8.6%) as the function number increases. This is because the PS has to wait for all functions to perform the gradient aggregation, and such a parameter synchronization [19] overhead cannot be overlooked as more functions are provisioned.

Can λDNN guarantee the objective DDNN training time? We evaluate the predictability of DDNN training performance under the naive [20], modified Siren [16], and λDNN resource provisioning strategies with two typical DNN models (*i.e.*, 1DCNN and ResNet50). Specifically, we train 5 epochs for 1DCNN and 1 epoch for ResNet50. We set three different objective training time as 90, 150, 210 seconds for 1DCNN and 600, 700, 800 seconds for ResNet50, respectively. As shown in Fig. 10, we observe that our λDNN strategy can leverage less provisioned function resources to guarantee the objective training time, as compared with the other two strategies. Though the modified Siren strategy can achieve the least DDNN training time, it over-provisions the function resources and thus degrades the function resource utilization as analyzed in Sec. 2.2. In addition, the naive strategy is likely to violate the objective training time as it

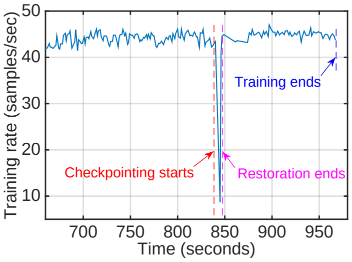

Fig. 12: Function training rate over time during MobileNet training with λ*DNN* as function timeout occurs.

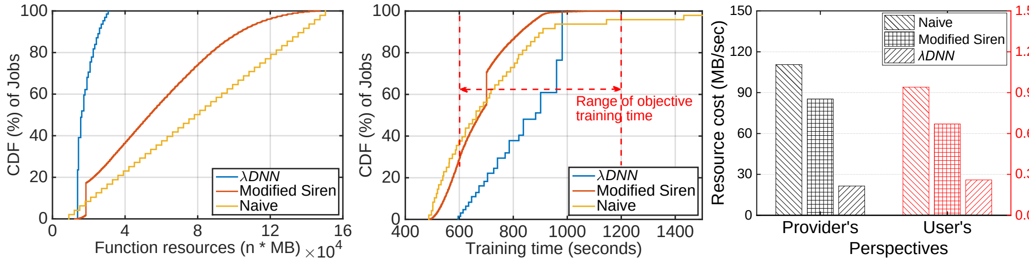

(a) (b) (c)

Fig. 13: CDF of (a) provisioned function resources and (b) DDNN training time of $117,325$ production jobs from Microsoft Azure trace, and (c) the benefits of λ*DNN* from the perspectives of both users and providers.

randomly selects provisioned function resources.

In more detail, with the objective time of 90 seconds for 1DCNN in Fig 10(a), the naive strategy always allocates the largest memory size (*i.e.,* $3,008$ MB) and randomly provisions 10 functions. The observed training time of such a provisioning plan is 53.6 seconds which is almost the same as that of another $(2,624,\ 8)$ provisioning plan (*i.e.,* $2,624$ MB memory and 8 functions) obtained by the modified Siren strategy. Though λ*DNN* achieves the largest model training time (*i.e.,* 86.2 seconds), it provisions the least amount of function resources $(1,088,\ 10)$ while completing the job before the objective training time. Our experiment results obtained on ResNet50 in Fig. 10(b) are similar to that on 1DCNN. As a result, over-provisioning function resources is likely to degrade the DDNN training performance and incur large monetary cost of provisioned function resources, which will be analyzed as follows.

Can λ*DNN* minimize the monetary cost of serverless functions? As shown in Fig. 11, we observe that λ*DNN* always achieves the minimum monetary cost of resource provisioning for DDNN training. Specifically, λ*DNN* can save the monetary cost by up to 19.7% and 57.9%, as compared with the naive [20] and modified Siren [16] provisioning strategies, respectively. Fig. 11(a) shows that the naive strategy has the largest monetary cost because it incurs resource over-provisioning $(3,008,\ 10)$ for 90 seconds or under-provisioning $(3,008,\ 1)$ for 210 seconds. As an example, though the naive strategy can save 38.7% training time under the objective training time of 90 seconds, its monetary cost is 57.9% higher than λ*DNN*. As shown in Fig. 11(b), the modified Siren still has higher monetary cost than λ*DNN* simply because it always over-provisions function resources, as we have illustrated in Fig 10(b). The rationale is that the modified Siren [16] adopts the DRL method, which highly depends on the quality of training data samples of DRL model. To achieve good performance, the modified Siren is likely to train DRL model for each DNN model using a number of data samples, while λ*DNN* builds a lightweight analytical performance model based on the workload profiling for each DNN model only once.

Can λ*DNN* handle the timeout of serverless functions? To extend the DDNN training time to exceeding 15 minutes, we set the training epochs of MobileNet model as 6, and its objective training time T_o as $1,200$ seconds. To guarantee the training performance, our λ*DNN* strategy provisions 7 functions with $1,728$ memory size, while the modified Siren [16] and naive [20] strategies provision 10 functions with $2,752$ memory size and 4 functions with $3,008$ memory size, respectively. The training time of MobileNet under λ*DNN* and modified Siren is 967.5 seconds and 738.9 seconds (both are within $1,200$ seconds), respectively, while the naive strategy cannot complete the DDNN training process because it does not handle the function timeout. In particular, the modified Siren over-provisions function resources compared with λ*DNN* so that the training process of MobileNet does not encounter the function timeout (within 900 seconds). Nevertheless, the modified Siren slightly incurs more monetary cost than λ*DNN* by 66.7%, and also the stock Siren [16] does not reveal the implementation details on dealing with the function timeout. In contrast, λ*DNN* leverages *proactive checkpointing* to deal with the function timeout, as elaborated in Sec. 4.2. As shown in Fig. 12, we observe that the function training rate is slightly impacted by our proactive checkpointing for around 6 seconds (*i.e.,* three iterations from 840 seconds to 846 seconds). As a result, λ*DNN* brings an acceptable checkpointing and restoration overhead to the DDNN training performance.

5.3 Large-scale Simulations Driven by Microsoft Azure Traces

To illustrate the benefits of λ*DNN from the perspectives of both cloud users and providers* and obtain complementary insights, we conduct large-scale simulations driven by the real-world deep learning job trace [30] from Microsoft Azure. Specifically, we set up our simulation environment using $117,325$ production deep learning jobs from the real-world trace, and $50,000$ functions with a maximum amount of $3,008$ memory. We randomly set the objective DDNN training time in the range from 600 to $1,200$ seconds, and we extract the `submitted_time` field in the production job trace [30] as the start time for each job in our simulation.

As shown in Fig. 13(a), we observe that the modified Siren [16] and naive [20] strategies significantly *over-provision* function resources (*i.e.,* the product of function number and memory size) to the jobs, while λ*DNN* provisions adequate function resources to guarantee the objective DDNN training time. Specifically, our simulation results reveal that λ*DNN* can cut down the amount of provisioned function resources by 68.5% and 77.2% on average for each job, compared with the modified Siren and naive strategies, respectively. Though the average training time for each job under λ*DNN* strategy is increased by 17.3% – 25.4% than the other two strategies, λ*DNN* can guarantee the objective DDNN training time (*i.e.,* the training time achieved by λ*DNN* is within the range from 600 to $1,200$ seconds), while the naive strategy violates the objective time goals for a number of jobs, as shown in Fig. 13(b). As revealed by our simulation results, the modified Siren and naive strategies complete the DDNN training before the objective time for 91.3% and 79.5% of jobs, respectively. In contrast, λ*DNN* can guarantee the objective training time for 99.98% of jobs. This is because the DRL method [16] relies on the quality of model training samples and its resource provisioning plans cannot guarantee the given objective time. In particular, λ*DNN* fails to guarantee the performance of 0.02% of training jobs in the trace, simply because the function resources are totally occupied by the current jobs and thus there lacks available resources for these jobs.

Based on our simulation analysis above, we further illustrate the benefits of λ*DNN* in Fig. 13(c) from the *perspectives of both cloud users and providers*. Specifically, we use the resource cost to represent the *unit cost* for serverless computing providers, which indicates the average amount of resources required to execute DDNN training workloads for one second. Under the circumstances of guaranteeing the objective training time, the less resource cost will make the provider save more function resources and serve more DDNN training requests. As an example in Fig. 10(b), to train ResNet50 within 800 seconds, the resource cost for the providers is 44.3 MB/sec, 36.2 MB/sec, and 24.3 MB/sec with the naive, modified Siren, and λ*DNN* strategies, respectively. Similarly in our trace-driven simulation, λ*DNN* can save the resource cost for the providers by 74.9% and 80.6% on average for each job, compared with the modified Siren and naive strategies, respectively. Meanwhile, we calculate the average monetary cost for serverless computing users, λ*DNN* can save the monetary cost by 60.7% and 72.1% on average for each job, compared with the modified Siren and naive strategies, respectively. Such a simulation result is consistent with our prototype experiments in Sec. 5.2.

5.4 Runtime Overhead of λ*DNN*

We evaluate the runtime overhead of λ*DNN* in terms of the profiling overhead of serverless DDNN training workloads and the computation time of λ*DNN* resource provisioning strategy (*i.e.,* Alg. 1). Specifically, we launch a Lambda function allocated with $3,008$ MB memory to profile the DDNN training workload. With a small set (*e.g.,* 2%) of data samples, we train each DNN model on the single launched function for 50 iterations. The profiling time for the training of `cifar10` DNN [27], 1DCNN [31], MobileNet [23], and ResNet50 models is 20.25, 15.72, 128.36, and 310.34 seconds, respectively. The result above shows that the profiling overhead highly depends on the type of DNN models and can be within several minutes. After obtaining the performance model parameters, we also run our λ*DNN* strategy in Alg. 1 on the single launched function. The computation overhead of λ*DNN* for `cifar10` DNN, 1DCNN, MobileNet, and ResNet50 models is 1.25, 1.38, 1.15, and 0.61 milliseconds, respectively. This is because the computation time of Alg. 1 is linear to the lower and upper bounds of the number and memory size of provisioned functions, as analyzed in Sec. 4.1. As a result, the runtime overhead of workload profiling is well controlled and the computation overhead of our λ*DNN* strategy is practically negligible.

6 Related Work

Performance characterization and optimization of serverless applications: There have been works on characterizing the function performance from the *user's perspective* (*i.e.,* outside of serverless platforms) [8]. For instance, two empirical studies are conducted on public serverless platforms such as AWS Lambda [4] and Azure Functions [6], in order to evaluate the performance of distributed data processing [32] and DNN inference workloads [29], respectively. To particularly optimize DDNN training performance, Feng *et al.* [33] design a multi-layer PS architecture with serverless functions to reduce the latency of transferring gradients. As functions cannot directly communicate with each other, however, such a hierarchical PS structure tends to bring much communication overhead to DDNN training. To tackle such function communication barriers, a recent work named Cirrus [20] deploys a cloud VM as the data store (*i.e.,* the PS) to facilitate the execution of end-to-end serverless machine learning workloads. λ*DNN* differs from prior works above in that: (1) We characterize serverless DDNN training performance in terms of PS network bandwidth, function CPU utilization, and local batch size. (2) We focus on guaranteeing DDNN training performance in serverless platforms, through the cost-efficient provisioning of function resources.

To particularly optimize the performance of serverless applications from the *provider's perspective* (*i.e.,* inside the serverless platforms), Shahrad *et al.* [34] fully identify a set of system-level performance overheads such as containerization, cold-start latency, and inter-function interference. To mitigate the performance overhead of function cold starts, Catalyzer [13] designs a generic serverless sandbox system to restore functions from the checkpoint image. Shahrad *et al.* [35] further optimize the keep-live value and pre-warm functions based on the invocation patterns of real-world function workloads. To provide resource isolation among functions, EMARS [36] designs a predictive model to limit the function memory size according to the workload usage, and FAASM [12] develops a lightweight isolation abstraction for data-intensive serverless computing. To achieve predictable performance for serverless applications, several works (*e.g.,* [37]) propose the centralized resource scheduler that can balance the load of functions [38], and dynamically allocates adequate amounts of CPU and memory resources to functions [39]. Orthogonal to prior works above, λ*DNN* focuses on optimizing the function resource provisioning plans to deliver predictable performance to serverless DDNN training workloads from the user's perspective, while reducing the resource cost from the provider's perspective. Besides, we experimentally identify *negligible* function performance interference in AWS Lambda [4].

Resource provisioning of serverless functions: There have been several recent studies devoted to provisioning adequate function resources to serverless applications. For example, an open-source resource provisioning tool named AWS Lambda Power Tuning [40] leverages Step Functions[5] to help users fine-tune the optimal memory allocation of Lambda functions. However, it requires running the user's workload with all the possible memory configurations, which inevitably brings non-negligible profiling overhead.

5. https://aws.amazon.com/step-functions/

To improve the cost efficiency of resource provisioning, MArk [15] and SplitServe [17] jointly provision VM instances and serverless functions for machine learning inference workloads and complex workloads (*e.g.,* Spark jobs), respectively. To meet the workload delay constraint and minimize user budget, COSE [18] leverages Bayesian Optimization to find the optimal memory size for serverless functions, while *λDNN* relies on a simple analytical performance model to find cost-efficient serverless resources solely for DDNN training workloads. To optimize the performance of machine learning training workloads under a given budget in serverless platforms, a more recent work named Siren [16] adopts the DRL method to dynamically adjust the number and memory size of provisioned functions. Our work differs from Siren [16] in that: (1) Siren relies on a black-box method (*i.e.,* DRL) to provision serverless functions, while *λDNN* explicitly builds an analytical model to predict DDNN training performance. (2) Siren stores model parameters in the shared storage (*e.g.,* S3), where the gradient aggregation cannot be directly calculated and thus causes non-negligible model update overhead. (3) *λDNN* explicitly considers the performance degradation caused by the PS resource bottleneck and inadequate small local batch size, which severely impacts the function CPU utilization in serverless platforms.

Cache management in serverless platforms: Several works focus on designing a cache storage system to facilitate the communication among functions. For example, Pocket [41] leverages the storage of different VM instance types to build a cost-effective ephemeral storage system for serverless applications. Locus [42] judiciously combines the slow but cheap storage (*i.e.,* Amazon S3 [21]) and fast but expensive storage (*i.e.,* Redis) to achieve the best performance with lower cost for serverless analytics jobs. Instead of AWS S3 and ElastiCache[6], a recent work [25] designs an elastic cost-effective caching system named InfiniCache, which leverages the ephemeral serverless function memory resources to cache objects in the cloud. Orthogonal to the prior works above, *λDNN* can adopt these caching systems to make serverless DDNN training more cost-effective.

Performance modeling of DDNN Training: A number of works are devoted to predicting DDNN training performance. For example, Yan *et al.* [43] and *Paleo* [44] both build a fine-grained model to predict the training time of DNN models using a set of factors like DNN architecture, choices of parallelism methods and hardware, as well as communications strategies. Without a prior knowledge of the training model and hardware, *Optimus* [22] and CM-DARE [45] build a resource-performance regression model by online fitting the training speed. However, such model fitting brings non-negligible overhead and the model accuracy relies on the quality of fitting data samples. A more recent work named *Cynthia* [2] predicts the DDNN training performance in cloud VMs by considering the CPU and network bandwidth bottleneck and hardware heterogeneity. Different from prior works above, our performance model in *λDNN* builds a *high-level* DDNN training performance model which solely works in serverless platforms, by leveraging the PS network bandwidth and function CPU utilization.

6. https://aws.amazon.com/elasticache/

7 Conclusion

To achieve predictable performance and save the training budget for serverless DDNN training workloads, this paper presents the design and implementation of *λDNN*, a cost-efficient function resource provisioning framework in serverless platforms. Leveraging the network bandwidth of PS and function CPU utilization, *λDNN* builds a lightweight analytical DDNN training performance model, which explicitly considers the performance degradation caused by the resource bottleneck of PS and small local batch size. Based on such a performance model, *λDNN* is able to provision an adequate number and memory size of functions to train the DNN model within an objective training time, while minimizing the monetary cost of provisioned function resources. Extensive prototype experiments on AWS Lambda and large-scale trace-driven simulations demonstrate that, *λDNN* can achieve predictable DDNN training performance and save the monetary cost of provisioned functions by up to 66.7%, in comparison to the state-of-the-art function resource provisioning strategies.

References

[1] J. Verbraeken, M. Wolting, J. Katzy, J. Kloppenburg, T. Verbelen, and J. S. Rellermeyer, "A Survey on Distributed Machine Learning," *ACM Computing Surveys*, vol. 53, no. 2, pp. 1–33, 2020.
[2] H. Zheng, F. Xu, L. Chen, Z. Zhou, and F. Liu, "Cynthia: Cost-Efficient Cloud Resource Provisioning for Predictable Distributed Deep Neural Network Training," in *Proc. of ICPP*, Aug. 2019, pp. 1–11.
[3] E. Jonas, J. Schleier-Smith, V. Sreekanti, C.-C. Tsai, A. Khandelwal, Q. Pu, V. Shankar, J. Carreira, K. Krauth, N. Yadwadkar *et al.*, "Cloud Programming Simplified: A Berkeley View on Serverless Computing," *arXiv preprint arXiv:1902.03383*, 2019.
[4] AWS Lambda. [Online]. Available: https://aws.amazon.com/lambda/
[5] Google Cloud Functions. [Online]. Available: https://cloud.google.com/functions/
[6] Azure Functions. [Online]. Available: https://azure.microsoft.com/en-us/services/functions/
[7] X. C. Lin, J. E. Gonzalez, and J. M. Hellerstein, "Serverless Boom or Bust? An Analysis of Economic Incentives," in *Proc. of USENIX HotCloud*, Jul. 2020.
[8] L. Wang, M. Li, Y. Zhang, T. Ristenpart, and M. Swift, "Peeking Behind the Curtains of Serverless Platforms," in *Proc. of USENIX ATC*, Jul. 2018, pp. 133–146.
[9] V. Sreekanti, C. Wu, S. Chhatrapati, J. E. Gonzalez, J. M. Hellerstein, and J. M. Faleiro, "A Fault-Tolerance Shim for Serverless Computing," in *Proc. of Eurosys*, Apr. 2020, pp. 1–15.
[10] A. Or, H. Zhang, and M. J. Freedman, "Resource Elasticity in Distributed Deep Learning," in *Proc. of MLSys*, Mar. 2020, pp. 1–12.
[11] A. Agache, M. Brooker, A. Florescu, A. Iordache, A. Liguori, R. Neugebauer, P. Piwonka, and D.-M. Popa, "Firecracker: Lightweight Virtualization for Serverless Applications," in *Proc. of USENIX NSDI*, Feb. 2020, pp. 419–434.
[12] S. Shillaker and P. Pietzuch, "FAASM: Lightweight Isolation for Efficient Stateful Serverless Computing," in *Proc. of USENIX ATC*, Jul. 2020.
[13] D. Du, T. Yu, Y. Xia, B. Zang, G. Yan, C. Qin, Q. Wu, and H. Chen, "Catalyzer: Sub-millisecond Startup for Serverless Computing with Initialization-less Booting," in *Proc. of ACM ASPLOS*, Mar. 2020, pp. 467–481.
[14] E. van Eyk, A. Iosup, C. L. Abad, J. Grohmann, and S. Eismann, "A SPEC RG Cloud Group's Vision on the Performance Challenges of FaaS Cloud Architectures," in *Proc. of ACM ICPE*, Apr. 2018, pp. 21–24.
[15] C. Zhang, M. Yu, W. Wang, and F. Yan, "MArk: Exploiting Cloud Services for Cost-Effective, SLO-Aware Machine Learning Inference Serving," in *Proc. of USENIX ATC*, Jul. 2019, pp. 1049–1062.
[16] H. Wang, D. Niu, and B. Li, "Distributed Machine Learning with a Serverless Architecture," in *Proc. of IEEE Infocom*, Apr. 2019, pp. 1288–1296.

[17] A. Jain, A. F. Baarzi, N. Alfares, G. Kesidis, B. Urgaonkar, and M. Kandemir, "SplitServe: Efficiently Splitting Complex Workloads Across FaaS and IaaS," in *Proc. of ACM SOCC*, Nov. 2019, pp. 487–487.
[18] N. Akhtar, A. Raza, V. Ishakian, and I. Matta, "COSE: Configuring Serverless Functions using Statistical Learning," in *Proc. of IEEE Infocom*, Apr. 2020, pp. 1–10.
[19] K. Mahajan, A. Balasubramanian, A. Singhvi, S. Venkataraman, A. Akella, A. Phanishayee, and S. Chawla, "Themis: Fair and Efficient GPU Cluster Scheduling," in *Proc. of USENIX NSDI*, Feb. 2020, pp. 289–304.
[20] J. Carreira, P. Fonseca, A. Tumanov, A. Zhang, and R. Katz, "Cirrus: a Serverless Framework for End-to-end ML Workflows," in *Proc. of ACM SOCC*, Nov. 2019, pp. 13–24.
[21] AWS S3. [Online]. Available: https://aws.amazon.com/s3/
[22] Y. Peng, Y. Bao, Y. Chen, C. Wu, and C. Guo, "Optimus: an efficient dynamic resource scheduler for deep learning clusters," in *Proc. of EuroSys*, Apr. 2018, pp. 1–14.
[23] MobileNet and MobileNetV2. [Online]. Available: https://keras.io/api/applications/mobilenet/
[24] ResNet and ResNetV2. [Online]. Available: https://keras.io/api/applications/resnet/
[25] A. Wang, J. Zhang, X. Ma, A. Anwar, L. Rupprecht, D. Skourtis, V. Tarasov, F. Yan, and Y. Cheng, "InfiniCache: Exploiting Ephemeral Serverless Functions to Build a Cost-Effective Memory Cache," in *Proc. of USENIX FAST*, Feb. 2020, pp. 267–281.
[26] D. A. Freedman, *Statistical Models: Theory and Practice*. Cambridge University Press, 2009.
[27] Tensorflow tutorials: CIFAR-10. [Online]. Available: https://github.com/tensorflow/models/tree/master/tutorials/image/cifar10
[28] S. Boyd and L. Vandenberghe, *Convex Optimization*. Cambridge University Press, 2004.
[29] V. Ishakian, V. Muthusamy, and A. Slominski, "Serving Deep Learning Models in A Serverless Platform," in *Proc. of IEEE IC2E*, Apr. 2018, pp. 257–262.
[30] M. Jeon, S. Venkataraman, A. Phanishayee, J. Qian, W. Xiao, and F. Yang, "Analysis of Large-Scale Multi-Tenant GPU Clusters for DNN Training Workloads," in *Proc. of USENIX ATC*, Jul. 2019, pp. 947–960.
[31] 1D CNN for text classification. [Online]. Available: https://keras.io/examples/imdb_cnn/
[32] H. Lee, K. Satyam, and G. C. Fox, "Evaluation of Production Serverless Computing Environments," in *Proc. of IEEE CLOUD*, Jul. 2018, pp. 827–830.
[33] L. Feng, P. Kudva, D. D. Silva, and J. Hu, "Exploring serverless computing for neural network training," in *Proc. of IEEE CLOUD*, Dec. 2018, pp. 334–341.
[34] M. Shahrad, J. Balkind, and D. Wentzlaff, "Architectural Implications of Function-as-a-Service Computing," in *Proc. of Micro*, Oct. 2019, pp. 1063–1075.
[35] M. Shahrad, R. Fonseca, Í. Goiri, G. Chaudhry, P. Batum, J. Cooke, E. Laureano, C. Tresness, M. Russinovich, and R. Bianchini, "Serverless in the Wild: Characterizing and Optimizing the Serverless Workload at a Large Cloud Provider," in *Proc. of USENIX ATC*, Jul. 2020.
[36] A. Saha and S. Jindal, "EMARS: Efficient Management and Allocation of Resources in Serverless," in *Proc. of IEEE CLOUD*, Jul. 2018, pp. 827–830.
[37] K. Kaffes, N. J. Yadwadkar, and C. Kozyrakis, "Centralized Coregranular Scheduling for Serverless Functions," in *Proc. of ACM SOCC*, Nov. 2019, pp. 158–164.
[38] A. Singhvi, K. Houck, A. Balasubramanian, M. D. Shaikh, S. Venkataraman, and A. Akella, "Archipelago: A Scalable Low-Latency Serverless Platform," *arXiv preprint arXiv:1911.09849*, 2019.
[39] M. R. HoseinyFarahabady, A. Y. Zomaya, and Z. Tari, "A Model Predictive Controller for Managing QoS Enforcements and Microarchitecture-Level Interferences in a Lambda Platform," *IEEE Transactions on Parallel and Distributed Systems*, vol. 29, no. 7, pp. 1442–1455, 2018.
[40] AWS Lambda Power Tuning. [Online]. Available: https://github.com/alexcasalboni/aws-lambda-power-tuning
[41] A. Klimovic, Y. Wang, P. Stuedi, A. Trivedi, J. Pfefferle, and C. Kozyrakis, "Pocket: Elastic Ephemeral Storage for Serverless Analytics," in *Proc. of USENIX OSDI*, Oct. 2018, pp. 427–444.
[42] Q. Pu, S. Venkataraman, and I. Stoica, "Shuffling, Fast and Slow Scalable Analytics on Serverless Infrastructure," in *Proc. of USENIX NSDI*, Feb. 2019, pp. 193–206.
[43] F. Yan, O. Ruwase, Y. He, and T. Chilimbi, "Performance Modeling and Scalability Optimization of Distributed Deep Learning Systems," in *Proc. of ACM SIGKDD*, Aug. 2015, pp. 1355–1364.
[44] H. Qi, E. R. Sparks, and A. Talwalkar, "Paleo: A performance model for deep neural networks," in *Proc. of ICLR*, Apr. 2017.
[45] S. Li, R. J. Walls, and T. Guo, "Characterizing and Modeling Distributed Training with Transient Cloud GPU Servers," in *Proc. of ICDCS*, Jul. 2020, pp. 1–11.

Fei Xu received the PhD degree in computer science and engineering from the Huazhong University of Science and Technology, Wuhan, China, in 2014. He received Outstanding Doctoral Dissertation Award in Hubei province, China, and ACM Wuhan & Hubei Computer Society Doctoral Dissertation Award in 2015. He is currently an associate professor with the School of Computer Science and Technology, East China Normal University, Shanghai, China. His research interests include cloud computing and datacenter, virtualization technology, and distributed systems.

Yiling Qin is currently working toward the master's degree in the School of Computer Science and Technology, East China Normal University, Shanghai, China. Her research interests focus on cloud computing and distributed machine learning systems.

Li Chen received the BEngr degree from the Department of Computer Science and Technology, Huazhong University of Science and Technology, China, in 2012 and the MASc degree from the Department of Electrical and Computer Engineering, University of Toronto, in 2014 and the PhD degree in computer science and engineering from the Department of Electrical and Computer Engineering, University of Toronto, in 2018. She is currently an assistant professor with the Department of Computer Science, School of Computing and Informatics, University of Louisiana at Lafayette, Lafayette, USA. Her research interests include big data analytics systems, cloud computing, datacenter networking, and resource allocation.

Zhi Zhou received the BS, ME, and PhD degrees all from the School of Computer Science and Technology, Huazhong University of Science and Technology (HUST), Wuhan, China, in 2012, 2014, and 2017, respectively. He is currently a research associate fellow with the School of Data and Computer Science, Sun Yat-sen University, Guangzhou, China. In 2016, he has been a visiting scholar with the University of Gottingen. His research interests include edge computing, cloud computing, and distributed systems. He is a member of the IEEE.

Fangming Liu (S'08, M'11, SM'16) received the B.Eng. degree from the Tsinghua University, Beijing, and the Ph.D. degree from the Hong Kong University of Science and Technology, Hong Kong. He is currently a Full Professor with the Huazhong University of Science and Technology, Wuhan, China. His research interests include cloud computing and edge computing, datacenter and green computing, SDN/NFV/5G and applied ML/AI. He received the National Natural Science Fund (NSFC) for Excellent Young Scholars, and the National Program Special Support for Top-Notch Young Professionals. He is a recipient of the Best Paper Award of IEEE/ACM IWQoS 2019, ACM e-Energy 2018 and IEEE GLOBECOM 2011, as well as the First Class Prize of Natural Science of Ministry of Education in China.